Transient transport in III-nitrides: interplay of momentum and energy relaxation times

2007 J. Phys.: Condens. Matter 19 346214

(http://iopscience.iop.org/0953-8984/19/34/346214)

IOP PUBLISHING JOURNAL OF PHYSICS: CONDENSED MATTER

J. Phys.: Condens. Matter **19** (2007) 346214 (13pp) doi:10.1088/0953-8984/19/34/346214

Transient transport in III-nitrides: interplay of momentum and energy relaxation times

Clóves G Rodrigues[1], Áurea R Vasconcellos[2], Roberto Luzzi[2] and Valder N Freire[3]

[1] Núcleo de Pesquisa em Física, Departamento de Física, Universidade Católica de Goiás, 74605-010, Goiânia, Goiás, Brazil
[2] Instituto de Física 'Gleb Wataghin', Universidade Estadual de Campinas, UNICAMP, 13083-970, Campinas, São Paulo, Brazil
[3] Departamento de Física, Universidade Federal do Ceará, Campus do Pici, 60455-760 Fortaleza, Ceará, Brazil

Received 9 November 2006, in final form 23 May 2007
Published 24 July 2007
Online at stacks.iop.org/JPhysCM/19/346214

Abstract

The ultrafast transient transport in wide-gap polar III-nitride semiconductors in electric fields is considered. A nonlinear and time-dependent (on the evolution of the nonequilibrium-irreversible thermodynamic state of the system) Drude-like law is derived, with the conductivity related to a so-called transport time (or current characteristic time which is related to a memory-dependent momentum relaxation time). From the collision operators, present in the evolution equations for the carriers' energy and momentum, are obtained quantities playing the role of time-dependent energy and momentum relaxation times. The electron drift velocity overshoot at intermediate-intensity fields in GaN, AlN and InN is evidenced, and its onset is explained as a result of the interplay of momentum and energy relaxation times.

1. Introduction

The recent successful commercialization of III-nitride-based light-emitting diodes in the blue–yellow range, and the development of injection lasers and ultraviolet detectors, initially drove the focus of basic research on these wide-gap semiconductors to the understanding of their optical properties [1–4]. However, soon their favourable properties for the implementation of electronic-power devices, high-performance and high-frequency transistors [5–9], with superior characteristics than those based on silicon [10, 11], was also recognized. The efforts undertaken in the investigation of the III-nitride steady-state transport properties, looking for a better determination of bulk material parameters and band structure [12], are relevant for establishing their figure of merit for electronic devices with certain confidence. However, despite the improved understanding of the steady-state transport properties of III-nitrides obtained in the last few years, the agreement of the carriers' mobility data with theoretical

descriptions varies from broad to very good [13]; only a qualitative agreement was obtained between theoretical predictions and the recent measurements of the electron velocity-field characteristics in GaN [14].

Focus on the improvement of III-nitride-based devices with submicron channels has stimulated research on their transient–transport properties, since in this case the carriers may not attain the steady-state transport regime. The possibility of transient ballistic transport in GaN was demonstrated to occur for applied electric fields greater than 140 kV cm^{-1} [15], and investigations on the transient–transport regime, have indicated the possibility of existence of an overshoot effect in both the electron drift velocity [16–19] and mean energy [19]. In the work of [19], the explanation for the existence of the overshoot effect in the III-nitrides, in conditions where intervalley scattering is negligible, was considered to be due to the interplay of energy and momentum relaxation times: no overshoot occurs when the momentum relaxation time, which is smaller than the energy relaxation time shortly after application of the electric field, becomes predominantly larger than the other; on the other hand, the overshoot follows at intermediate to high fields when the relaxation time for energy remains larger than the one for momentum. But, no detailed explanation was presented confirming the validity of the above arguments.

In this paper we present one such detailed derivation, obtaining analytical expressions for the so-called characteristic time for conduction (or current) and the momentum relaxation time, from which the conditions for the onset of the electron drift velocity overshoot, in the case of these polar semiconductors in the parabolic conduction-band approximation, can be clearly evidenced. For that purpose we obtain the equations of evolution for the energy of electrons and longitudinal-optic and acoustic phonons, $E_c(t)$, $E_{LO}(t)$, $E_{AC}(t)$ (the transverse-optic phonons are ignored, since they weakly interact with the electrons in the conduction band), and the electrons' momentum $\mathbf{P}(t)$. They are built within the framework of a nonequilibrium statistical ensemble formalism (NESEF for short [20]), which provides an elegant, practical, and physically clear picture for describing irreversible processes [21], as for example in semiconductors far from equilibrium, which is the case considered here.

It can be noticed that the theory of transport went through different approaches along the past century, in a continuous process of improvement (the origin goes back to the fundamental work of the great Ludwig Boltzmann). Such approaches have been classified by Robert Zwanzig in [22]. At present we may mention the two at the front line, namely, the nonequilibrium molecular dynamics (NMD for short), and the kinetic theory based on the NESEF, as indicated above. In particular, NMD is in the present case referred to as the Monte Carlo approach. Both approaches have advantages and shortcomings in their general formulation, but in the case of charge transport in semiconductors (as it the one treated here) they appear as equivalent in the sense of providing, for several cases considered, numerical results that are very similar: some examples are presented in [23]. The NESEF-based transport theory as here used can be considered as a particular formulation of Boltzmann's original theory [24] involving a kind of Grad's moment approach of solution [25]. It is a result of averaging over the nonequilibrium statistical ensemble the mechanical Heisenberg equations of motion for the observables relevant for the problem in hand. Zwanzig stated that the formalism has by far the most appealing structure and may become the most effective method for dealing with nonlinear transport process [22].

Through the numerical solution of the associated nonlinear quantum transport equations based on the NESEF, we characterize the conditions for the onset of the electron velocity overshoot in wurtzite GaN, AlN, and InN in the presence of electric fields of low to intermediate intensities, when it is possible to neglect intervalley electron scattering effects, which are present at high fields. We have estimated these limiting values as being of the order of

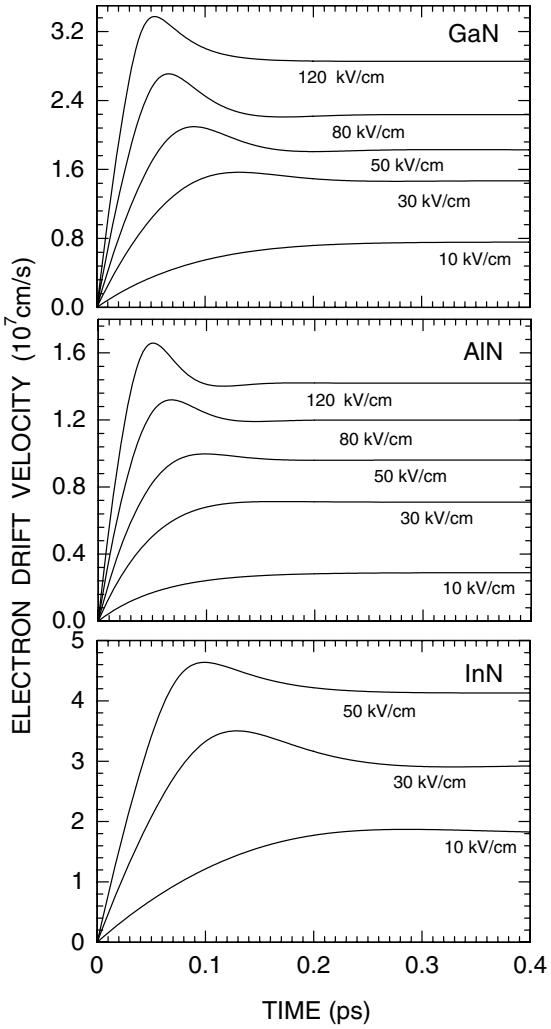

Figure 1. Evolution towards the steady state of the electron drift velocity in GaN (top), AlN (middle), and InN (bottom).

120 kV cm^{-1} for GaN and AlN, and 50 kV cm^{-1} for InN (see figures 1 and 2): these values are confirmed for the cases of GaN and InN analysed in the work of Starikov *et al* [26], who are using a Monte Carlo approach (see figures 1 and 2 in [26]). In all these domains of values of the electric field the differential conductivity is monotonically increasing with the electric field strength.

We obtain clear conditions for the overshoot onset of both the electron drift velocity and the quasitemperature in GaN, AlN and InN for electric field strengths higher than 20 kV cm^{-1}, 40 kV cm^{-1}, and 20 kV cm^{-1}, respectively.

2. Momentum and energy relaxation times

The study of transport properties of semiconductors under high level of excitation, eventually following nonlinear laws, is of great interest not only for its relevance in the functioning of

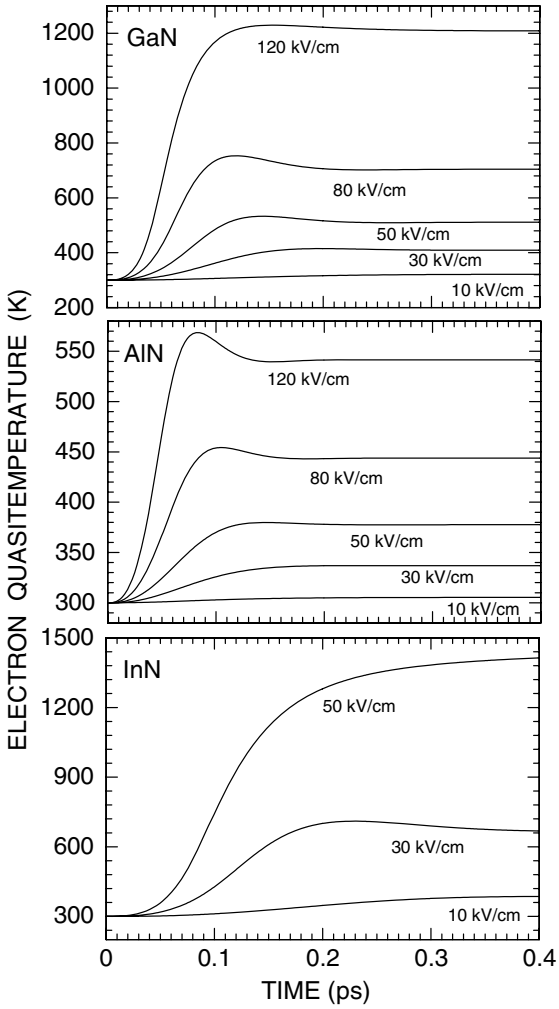

Figure 2. Evolution towards the steady state of the electron nonequilibrium temperature in GaN (top), AlN (middle), and InN (bottom).

electronic and optoelectronic devices, but also because of providing an excellent testing ground for theoretical ideas in the field of many-body systems in far-from-equilibrium conditions, as we do here. In particular, nonlinearities that are present in both transport properties and relaxation processes may give origin to new and interesting phenomena. As a general rule this question of transport and optical properties of carriers (whose origin is in doping, type n or p, or photoinjection when a double plasma of electrons and holes is produced) has been usually dealt with by Monte Carlo computational methods. For the reasons stated before, we resort here to the use of an analytical kinetic theory of a broad scope, the above-mentioned one based on a nonequilibrium statistical ensemble formalism.

We consider the case of polar semiconductors described by a parabolic conduction-band model (within the effective mass approximation, and ignoring conduction-band secondary valleys—hence an upper limit on the strength of the electric field needs to be imposed, as shown below), where a concentration of electrons, n, has been created by doping. A constant

electric field of strength $\mathcal{E}$ in, say, the x-direction is applied, which accelerates these carriers ('hot' carriers since the electric field drives them in the hot electron transport regime [27]), while there follows a transferring of their energy and momentum (in excess of equilibrium) to the phonon field. The sample is in contact with a thermal reservoir at temperature T_0, with the phonons being warmed up in scattering events involving Fröhlich, deformation potential, and piezoelectric interactions with the hot carriers; scattering by impurities is also considered.

First we note that the Hamiltonian of the system is written as $\hat{H} = \hat{H}_0 + \hat{H}_1$, where $\hat{H}_0$ consists of the free Hamiltonians of the electrons and of the phonons, while $\hat{H}_1$ contains the electron–phonon interactions, the anharmonic interactions among the phonons, and the coupling with the external electric field. Coulomb interaction between carriers (contributing to very fast—subpicosecond scale—relaxation processes) is incorporated in the random-phase approximation. According to the formalism [20, 21], we need to choose the set of basic variables which describes the macroscopic state of the system in the given conditions. The first two basic variables are taken as the free Hamiltonians (the one of the electrons, $\hat{H}_e$, and those of the longitudinal-optic and acoustical phonons, $\hat{H}_{LO}$ and $\hat{H}_{AC}$, respectively) and the number of electrons, $\hat{N}_e$. Next, on account that the electric field produces a current, it is introduced the electrons' linear momentum $\hat{\mathbf{P}}_e$ (which is the flux of mass). The associated set of basic macrovariables (that is, those which characterize the nonequilibrium thermodynamic state of the system) are the average value of the dynamical quantities indicated above over the corresponding nonequilibrium ensemble. They are denoted by

$$\{E_e(t), N_e(t), \mathbf{P}_e(t), E_{LO}(t), E_{AC}(t)\}, \tag{1}$$

and an equivalent thermodynamic representation can be done in terms of the associated Lagrange multipliers that the variational method NESEF introduces, which constitute a set of intensive nonequilibrium thermodynamic variables for which we write

$$\{\beta_e(t), -\beta_e(t)\mu_e^*(t), -\beta_e(t)\mathbf{v}_e(t), \beta_{LO}(t), \beta_{AC}(t)\}. \tag{2}$$

Here, $\beta_e^{-1}(t) = k_B T_e^*$, $\beta_\eta^{-1}(t) = k_B T_\eta^*(t)$, with $\eta =$ LO, AC, introducing the quasitemperatures (nonequilibrium temperatures of the 'hot' systems [20, 21, 28]) of electrons and of phonons in the different branches; $\mu_e^*(t)$ is the quasi-chemical potential, and $\mathbf{v}_e(t)$ the drift velocity.

We are now in a condition to derive the evolution of the nonequilibrium macroscopic state of the system by solving the corresponding kinetic equations for the basic variables of equation (1). We introduce the restriction of considering a good thermal contact of system and reservoir, such that the acoustic phonons remain constantly in equilibrium with the latter at temperature T_0 (which we take as 300 K). Hence, we need to consider the set of coupled equations of evolution given by

$$\frac{\mathrm{d}}{\mathrm{d}t}E_e(t) = -\frac{e\mathbf{E}}{m_e^*}\cdot\mathbf{P}_e(t) + J_{E_e}^{(2)}, \tag{3}$$

$$\frac{\mathrm{d}}{\mathrm{d}t}\mathbf{P}_e(t) = -Vn_e e\mathbf{E} + \mathbf{J}_{\mathbf{P}_e}^{(2)}, \tag{4}$$

$$\frac{\mathrm{d}}{\mathrm{d}t}E_{LO}(t) = J_{E_{LO}}^{(2)}(t) + \dot{E}_{LO,AN}(t), \tag{5}$$

where V is the volume of the sample. In equation (3) the first term on the right accounts for the rate of pumping of energy on the carrier system generated by the presence of the electric field, while the second, $J_{E_e}^{(2)}$, represents the rate of excess energy transferred to the lattice's LO phonons (the interactions with the acoustic phonons can be neglected). In equation (4) the first term on the right is the force produced by the presence of the electric field, and the second, $J_{\mathbf{P}_e}^{(2)}$ the rate of momentum transferred to the LO phonons. In equation (5) we have the

term of gain of energy pumped on the LO phonons by the 'hot' carriers, $J^{(2)}_{E_{\rm LO}}$, and the transfer, via anharmonic effects, of such energy to the AC phonons (at temperature T_0), $\dot{E}_{\rm LO,AN}(t)$, the latter acting as a thermal bath. The detailed expressions for the different collision operators are given elsewhere [29] (see the appendix); we recall that they are dependent on the intensive nonequilibrium thermodynamic variables of equation (2). Hence, the equations of evolution can be closed since the variables of equation (1), whose time derivatives appear on the left-hand side, are related to those thermodynamic variables of equation (2) via the equations (nonequilibrium equations of state in the NESEF-based statistical thermodynamics [20, 21])

$$E_{\rm e}(t) = \sum_{\mathbf{k}} (\hbar k^2/2m^*_{\rm e}) f^{\rm e}_{\mathbf{k}}(t) \simeq N_{\rm e}\left[\tfrac{3}{2}k_{\rm B}T^*_{\rm e}(t) + \tfrac{1}{2}m^*_{\rm e}v^2_{\rm e}(t)\right], \tag{6}$$

$$\mathbf{P}_{\rm e}(t) = \sum_{\mathbf{k}} \hbar\mathbf{k} f^{\rm e}_{\mathbf{k}}(t) \simeq N_{\rm e}m^*_{\rm e}\mathbf{v}_{\rm e}(t), \tag{7}$$

$$E_{\rm LO}(t) = \sum_{\mathbf{k}} \hbar\omega_{\mathbf{q},{\rm LO}}\nu_{\mathbf{q},{\rm LO}}(t) = \frac{V}{V_{\rm cell}}\hbar\omega_{\rm LO}\nu_{\rm LO}(t), \tag{8}$$

where $f^{\rm e}_{\mathbf{k}}(t) = {\rm Tr}\{c^\dagger_{\mathbf{k}}c_{\mathbf{k}}\rho(t)\} = [\exp\{\beta_{\rm e}(t)[\epsilon^{\rm e}_{\mathbf{k}} - \mu^*_{\rm e}(t) - \hbar\mathbf{k}\perp\mathbf{v}_{\rm e}(t)]\} + 1]^{-1}$, with $\epsilon^{\rm e}_{\mathbf{k}} = \hbar^2k^2/2m^*_{\rm e}$, and we have used the approximation

$$f^{\rm e}_{\mathbf{k}}(t) \simeq 4n_{\rm e}\left(\frac{\pi\hbar^2\beta_{\rm e}(t)}{2m^*_{\rm e}}\right)^{3/2} \exp\left\{-\frac{\beta_{\rm e}(t)}{2m^*_{\rm e}}(\hbar\mathbf{k} - m^*_{\rm e}\mathbf{v}_{\rm e}(t))^2\right\}, \tag{9}$$

valid in the usual experimental conditions [27, 29]. This is a time-dependent population which has a form resembling a drifted Maxwell–Boltzmann distribution, resulting from neglecting 1 in comparison with the exponential in the time-dependent Fermi–Dirac-like distribution indicated above. This is possible in the statistically nondegenerate-like limit, namely, when it is satisfied that $n\Lambda^3_T(t) \ll 1$, where $\Lambda_T(t) = \hbar/\sqrt{m^*k_{\rm B}T^*_{\rm e}(t)}$ is the thermal de Broglie wavelength. Moreover,

$$\nu_{\rm LO}(t) = {\rm Tr}\{b^\dagger b\rho(t)\} = [\exp\{\hbar\omega_{\rm LO}/k_{\rm B}T^*_{\rm LO}(t)\} - 1]^{-1}, \tag{10}$$

is the time-dependent population of LO phonons, where $\omega_{\rm LO}$ is the dispersionless frequency for LO phonons (Einstein model). Next, we define the time-dependent carrier-momentum, $\tau_{P_{\rm e}}(t)$, and carrier-energy, $\tau_{E_{\rm e}}(t)$, relaxation times given by

$$J^{(2)}_{P_{\rm e}}(t) \equiv -n_{\rm e}Vm^*_{\rm e}\frac{v_{\rm e}(t)}{\tau_{P_{\rm e}}(t)}, \tag{11}$$

$$J^{(2)}_{E_{\rm e}}(t) \equiv -\frac{E_{\rm e}(t) - E^{\rm eq}_{\rm e}}{\tau_{E_{\rm e}}(t)}, \tag{12}$$

where $v_{\rm e}(t)$ is the drift velocity in the direction of the electric field, and $E^{\rm eq}_{\rm e}$ the energy of the carriers in equilibrium with the AC phonons at temperature T_0, and the expressions for the relaxation times are given in the appendix.

Using equations (4), (7), and (11) we find an equation of evolution for the drift velocity, namely

$$\frac{\rm d}{{\rm d}t}\mathbf{v}_{\rm e}(t) = -(e/m^*_{\rm e})\mathbf{E} - \frac{\mathbf{v}_{\rm e}(t)}{\tau_{P_{\rm e}}(t)}, \tag{13}$$

which is an equation of the Newton–Langevin type, but with a time-dependent relaxation time (evolving in time with the macroscopic state of the system). Equation (13) can be alternatively written in the form of an integral equation, namely,

$$\mathbf{v}_{\rm e}(t) = -(e/m^*_{\rm e})\tau_{\rm ce}(t)\mathbf{E}, \tag{14}$$

where there is present what we call a characteristic time for conduction, namely

$$\tau_{ce}(t) = \exp\{-\Psi_e(t)\} \int_0^t \exp\{\Psi_e(t')\}dt', \tag{15}$$

with

$$\Psi_e(t) = \int_0^t dt'[\tau_{P_e}(t')]^{-1}, \tag{16}$$

which is a quantity depending, through $\tau_{P_e}(t)$, on $\beta_e(t)$ and $v_e(t)$ (cf equation (11)), and we have taken the initial condition $v_e(0) = 0$. Moreover, defining the current density

$$\mathbf{I}_e(t) = -n_e e\mathbf{v}_e(t), \tag{17}$$

after using equation (14), it takes the form

$$\mathbf{I}_e(t) = \sigma_e(t)\mathbf{E}, \tag{18}$$

where we have introduced a time-dependent Drude-type conductivity given by

$$\sigma_e(t) = (n_e e^2/m_e^*)\tau_{ce}(t). \tag{19}$$

Once again we stress that such time dependence comes from the evolution of the nonequilibrium state of the system; that is, $\sigma_e(t)$ and $\tau_{ce}(t)$ depend on $\beta_e(t)$ and $\mathbf{v}_e(t)$.

3. Explaining the onset of the drift velocity overshoot

For illustration let us consider the specific case of wurtzite-type GaN, AlN, and InN. We have used for these materials the characteristic parameters (effective mass, phonon frequencies, Fröhlich coupling strength, deformation potential strength, etc) available in the literature [18]. The electric field applied to GaN and AlN (InN) samples is restricted to be smaller than 120 kV cm^{-1} (60 kV cm^{-1}) since for higher field strengths the intervalley scattering, not considered in our calculations, can no longer be neglected. The doping concentration is taken as 1.0×10^{17} cm^{-3}, and a bath temperature of 300 K is used, which are the same as the values used by Foutz *et al* [18] in their calculations.

Figures 1 and 2 show the evolution of the electron drift velocity and quasitemperature, respectively, for several strengths of the applied electric field. These figures permit us to characterize the presence of an overshoot in both the electron drift velocity and quasitemperature for a high enough electric field strength. It can be noticed that the velocity overshoot occurs for fields higher than, roughly, 20 kV cm^{-1} in GaN, 40 kV cm^{-1} in AlN, and 20 kV cm^{-1} in InN. The intensity of the overshoot in the electron drift velocity is quite similar for all the III-nitrides, but it arises a little earlier ($\sim$0.05 ps) in GaN and AlN than in InN ($>$0.05 ps) for the same value of the electric field strength. The pattern of the overshoot in the electron quasitemperature is similar to that of the velocity overshoot, as can be noticed by comparing figures 1 and 2. Moreover, it is verified that the peak in the drift velocity follows in the time interval where the drift kinetic energy increases more rapidly than the thermal energy, and the peak in electron quasitemperature can be related to a minimum of the quotient of these two energies. The exception is when InN is subjected to a 50 kV cm^{-1} electric field such that as a result the intervalley scattering begins to become effective: at this point the calculation shows the emergence of a runaway effect which is a spurious one, resulting from the fact that in our calculations we have neglected side valleys, and therefore we cannot carry on the analysis beyond this point within the single-band valley model [29].

Pursuing the search for evidencing the conditions for the electron drift velocity overshoot, let us investigate the time evolution of the characteristic time for conduction (equation (15)) and

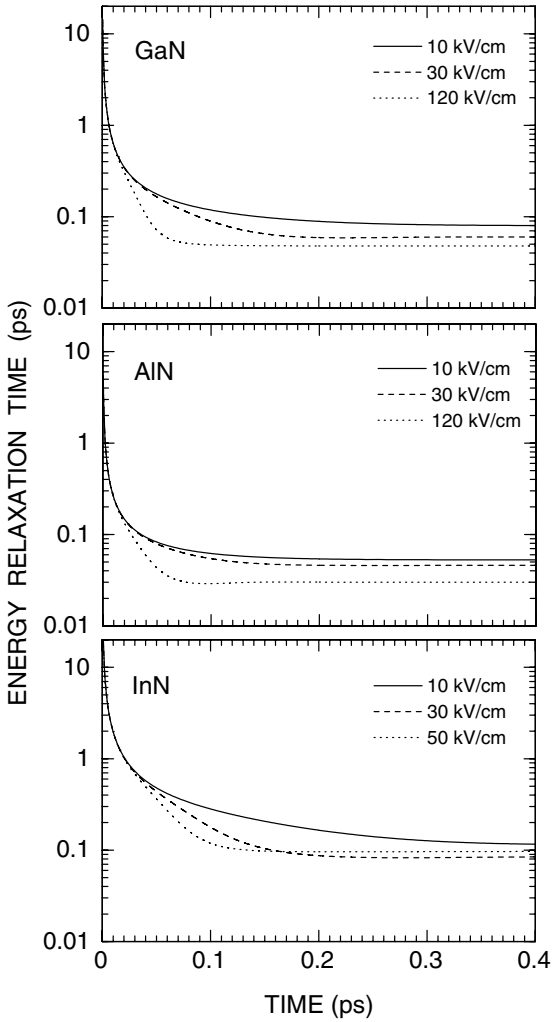

Figure 3. Evolution towards the steady state of the energy relaxation time for electrons in GaN (top), AlN (middle), and InN (bottom).

the momentum and energy relaxation times (see the appendix). Figure 3 shows the evolution of the energy relaxation time for the three III-nitrides we are analysing, which is monotonically decreasing and presents a similar behaviour for all the field strengths we have considered. This is also the case of the momentum relaxation time as shown in figure 4, which at low to intermediate fields varies smoothly. However, with increasing field strength the smooth behaviour changes to another one, which shows, for a threshold field strength, a very rapid (somewhat steep) decrease in the very earlier stages of evolution. This phenomenon is the one responsible for the onset of the overshoot in current, what can be characterized in the following way. At the maximum of the overshoot at, say, time $\bar{t}$, the time derivative of the electron drift velocity is null and the curvature (second derivative) is negative. Let us consider first the condition of the maximum, which implies that at $\bar{t}$

$$\left.\frac{\mathrm{d}}{\mathrm{d}t}\mathbf{v}_{\mathrm{e}}(t)\right|_{\bar{t}} = \frac{e}{m_{\mathrm{e}}^{*}}\mathbf{E} - \frac{\mathbf{v}_{\mathrm{e}}(\bar{t})}{\tau_{P_{\mathrm{e}}}(\bar{t})} = 0, \tag{20}$$

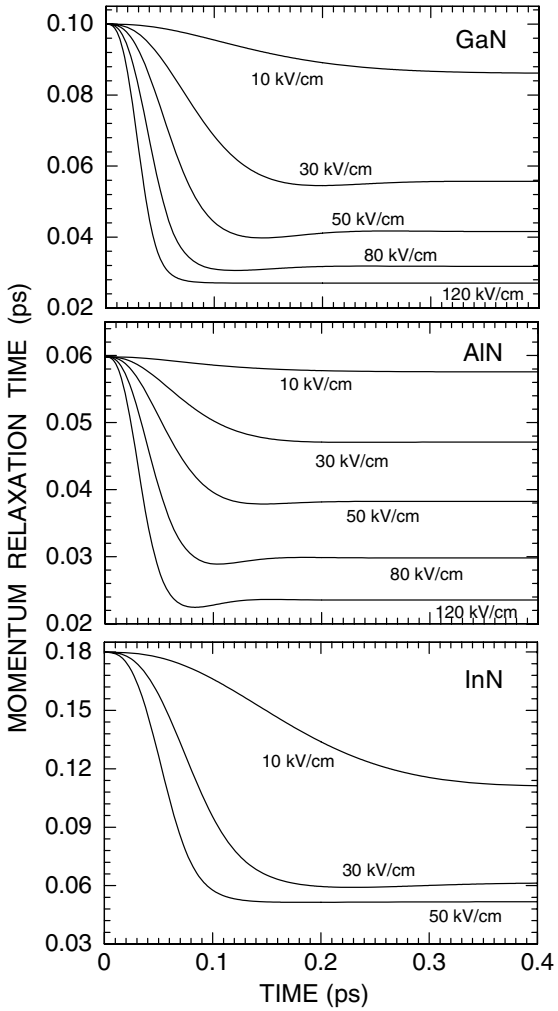

Figure 4. Evolution towards the steady state of the momentum relaxation time for electrons in GaN (top), AlN (middle), and InN (bottom).

according to equation (13). On the other hand, differentiating in time equation (14), we have at $t = \bar{t}$ that

$$\left.\frac{\mathrm{d}}{\mathrm{d}t}\mathbf{v}_{\mathrm{e}}(t)\right|_{\bar{t}} = \frac{e\mathbf{E}}{m_{\mathrm{e}}^{*}}\left.\frac{\mathrm{d}}{\mathrm{d}t}\tau_{\mathrm{ce}}(t)\right|_{\bar{t}} = 0, \tag{21}$$

but using equation (15) it follows that

$$\left.\frac{\mathrm{d}}{\mathrm{d}t}\tau_{\mathrm{ce}}(t)\right|_{\bar{t}} = -\frac{\tau_{\mathrm{ce}}(\bar{t})}{\tau_{P_{\mathrm{e}}}(\bar{t})} + 1 = 0, \tag{22}$$

and then, at $\bar{t}$,

$$\tau_{\mathrm{ce}}(\bar{t}) = \tau_{P_{\mathrm{e}}}(\bar{t}), \tag{23}$$

that is, the characteristic time for current and the momentum relaxation time are equal, and then overshoot can only follow in conditions allowing for them to cross (i.e. for sufficiently high values of the electric field strength).

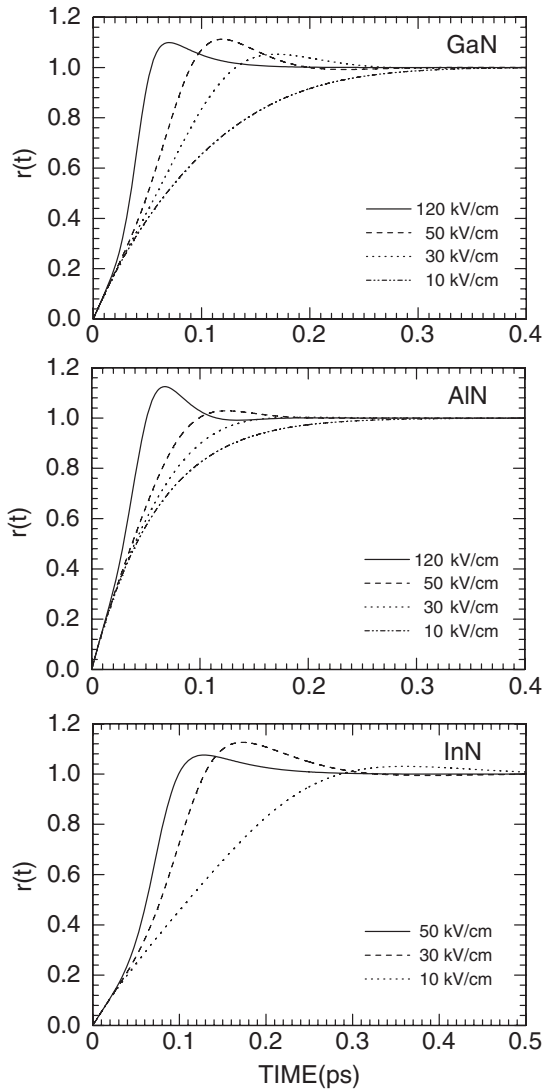

Figure 5. Evolution towards the steady state of the ratio $r(t)$ between the characteristic time for conduction (cf equation (15)) and the momentum relaxation time for electrons in GaN (top), AlN (middle), and InN (bottom).

In figure 5 is shown the ratio $r(t) = \tau_{ce}(t)/\tau_{P_e}(t)$, for five values of the electric field in the case of GaN and AlN, and three values in the case of InN. At low electric field strength such ratio increases monotonically, tending to the value 1 when the steady state is being achieved, and then the momentum relaxation time and the characteristic time for current coincide. It can be noticed that, in the earlier stages of evolution of the nonequilibrium macroscopic (thermodynamic) state of the system, at intermediate to high fields, the characteristic time for the current becomes larger than the momentum relaxation time, and there follows velocity overshoot. This is a result of the fact, already noticed on inspection of figure 5, that whereas the momentum relaxation time varies smoothly in time when in the presence of low to intermediate fields, at intermediate to strong fields it changes abruptly, decreasing in a subpicosecond time

scale. The transition from the, say, normal regime to one displaying overshoot occurs around a field of 20 kV cm^{-1} for GaN, 40 kV cm^{-1} for AlN, and 20 kV cm^{-1} for InN.

It can be noticed that at low fields the curvature of $v(t)$ is monotonically negative (convex) and smooth. But at higher fields, such that the condition for the emergence of overshoot is satisfied, the curvature at $\bar{t}$ is more and more pronounced for increasing field intensities, and afterwards the curvature changes from convex to concave. At the maximum curvature at $\bar{t}$,

$$\left.\frac{\mathrm{d}^2}{\mathrm{d}t^2}\tau_{\mathrm{ce}}(t)\right|_{\bar{t}} = -\left.\frac{1}{\tau_{P_{\mathrm{e}}}(\bar{t})}\frac{\mathrm{d}\tau_{\mathrm{ce}}(t)}{\mathrm{d}t}\right|_{\bar{t}} + \left.\frac{\tau_{\mathrm{ce}}(\bar{t})}{\tau^2_{P_{\mathrm{e}}}(\bar{t})}\frac{\mathrm{d}\tau_{P_{\mathrm{e}}}(t)}{\mathrm{d}t}\right|_{\bar{t}} < 0, \tag{24}$$

and since $\mathrm{d}\tau_{\mathrm{ce}}/\mathrm{d}t|_{\bar{t}} = 0$, it follows that

$$\left.\frac{\mathrm{d}\tau_{P_{\mathrm{e}}}(t)}{\mathrm{d}t}\right|_{\bar{t}} < 0, \tag{25}$$

and decreasing more rapidly with increasing field strength, thus increasing the (convex) curvature at the maximum of the overshoot. We recall that the changes in the momentum relaxation time are a consequence of the evolution of the nonequilibrium macrostate of the system, more precisely of the quasitemperatures of electrons and of optical LO phonons and of the drift velocity. Hence, the momentum relaxation time also depends indirectly on the energy relaxation time: the steep decrease of the momentum relaxation time in the earlier stages of evolution, when in the presence of intense fields, follows from, mainly, the strong 'heating' of the carriers and the 'warming' of the optical phonons, what enhances the scattering probability.

4. Concluding remarks

Shrinkage of the channel dimensions in III-nitride-based devices to a submicron scale (but beyond the 10 nm scale, where ballistic transport takes place [15]), imposes working conditions in which the transient transport characteristics would be important for contributing to a better performance. In a study of such transient characteristics, in the present work, resorting to the NESEF-based nonlinear quantum kinetic transport theory [20, 30], we derived the nonequilibrium time-dependent thermodynamic description of III-nitrides under electric fields of intermediate to strong strengths (<120 kV cm^{-1}), which allowed for a clear characterization of the drift velocity overshoot onset in terms of the interplay of momentum and energy relaxation times, which is not possible through Monte Carlo simulation or a Boltzmann-like balance equation in the momentum relaxation time approximation. Although disregarding intervalley scattering (which imposes limitations on the values of the field intensity to be used, as discussed in the text), the moderated electric field intensities drive the systems well in the hot-electron transport regime [27], described through an instantaneous and drifted Maxwell–Boltzmann-like distribution in which the electron quasitemperature ($\sim 10^3$ K; we recall that it is a measure in kelvin degrees of the energy pumped on the system by the external source [21, 28, 31]) is well above the temperature in equilibrium.

Within the parabolic band scheme approach, we have established clear conditions for overshoot onset of both the electron drift velocity and the quasitemperature in GaN, AlN, and InN for electric field strengths higher than 20 kV cm^{-1}, 40 kV cm^{-1}, and 20 kV cm^{-1}, respectively. Since the drift velocity at the overshoot peak is only about 20% higher than at its steady-state value, the possible contribution of the transient characteristics to the improvement of GaN, AlN (InN) nitride-based heterojunction field effect transistors should be very limited for electric fields smaller than 120 kV cm^{-1} (60 kV cm^{-1}). Finally, our work highlights the importance of considering evolution equations for the energy of longitudinal phonons in III-nitrides, without which it is not possible to evidence the smooth overshoot effect on the carriers' quasitemperature, and how it is related to the drift velocity overshoot.

Acknowledgments

We acknowledge financial support provided by the São Paulo State Research Agency (FAPESP) and the Brazilian National Research Council (CNPq) through the grant NanoBioEstruturas Project; ARV, VNF, and RL are CNPq Research Fellows.

Appendix. The relaxation times

The collision integral in equation (3), for the evolution of the energy, is given by [29]

$$J_E^{(2)} = \frac{2\pi}{\hbar}\sum_{\mathbf{k},\mathbf{q}} |M(\mathbf{q})|^2(\epsilon^{\mathrm{e}}_{\mathbf{k}+\mathbf{q}} - \epsilon^{\mathrm{e}}_{\mathbf{k}})[\nu_{\mathrm{LO}}(t) f^{\mathrm{e}}_{\mathbf{k}}(t)(1 - f^{\mathrm{e}}_{\mathbf{k}+\mathbf{q}}(t)) - f^{\mathrm{e}}_{\mathbf{k}+\mathbf{q}}(t)(1 + \nu_{\mathrm{LO}}(t))(1 - f^{\mathrm{e}}_{\mathbf{k}}(t))]\delta(\epsilon^{\mathrm{e}}_{\mathbf{k}+\mathbf{q}} - \epsilon^{\mathrm{e}}_{\mathbf{k}} - \hbar\omega_{\mathrm{LO}}), \tag{A.1}$$

where $\epsilon^{\mathrm{e}}_{\mathbf{k}} = \hbar^2k^2/2m^*_{\mathrm{e}}$, the population $f^{\mathrm{e}}_{\mathbf{k}}(t)$ is given in equation (9), $\nu_{\mathrm{LO}}(t)$ in equation (10), and $M(\mathbf{q})$ is the matrix element in Fröhlich interaction.

The collision in equation (4), for the evolution of the momentum, is given by [29]

$$\mathbf{J}^{(2)}_{\mathbf{P}_{\mathrm{e}}} = \frac{2\pi}{\hbar}\sum_{\mathbf{k},\mathbf{q}} \hbar\mathbf{q}|M(\mathbf{q})|^2[\nu_{\mathrm{LO}}(t) f^{\mathrm{e}}_{\mathbf{k}}(t)(1 - f^{\mathrm{e}}_{\mathbf{k}+\mathbf{q}}(t)) - f^{\mathrm{e}}_{\mathbf{k}+\mathbf{q}}(t)(1 + \nu_{\mathrm{LO}}(t)) \times (1 - f^{\mathrm{e}}_{\mathbf{k}}(t))] \times \delta(\epsilon^{\mathrm{e}}_{\mathbf{k}+\mathbf{q}} - \epsilon^{\mathrm{e}}_{\mathbf{k}} - \hbar\omega_{\mathrm{LO}}). \tag{A.2}$$

We recall that these results follows from the NESEF-based nonlinear quantum kinetic theory [20, 30], but they are given in the lowest order in the interaction strength which consists in taking the Markovian approximation in the theory [20, 30, 32]. It can be noticed that they have the form of the Golden Rule of Quantum Mechanics but averaged over the time-dependent nonequilibrium statistical ensemble.

Going from the sum in $\mathbf{k}$ to integration and performing the calculation, it follows that

$$J^{(2)}_{E_{\mathrm{e}}}(t) = nV(e\omega_{\mathrm{LO}})^2\sqrt{2m^*_{\mathrm{e}}/\pi k_{\mathrm{B}}T^*_{\mathrm{e}}(t)}\left(\frac{1}{\epsilon_\infty} - \frac{1}{\epsilon_0}\right)\exp\{z(t)/2\} \times [\nu_{\mathrm{LO}}(t) - (1 + \nu_{\mathrm{LO}}(t)) \times \exp\{-z(t)\}]K_0(z(t)/2), \tag{A.3}$$

and

$$\mathbf{J}^{(2)}_{\mathbf{P}_{\mathrm{e}},\mathrm{PO}}(t) = \sqrt{2/9\pi}nV(e\omega_{\mathrm{LO}})^2(m^*_{\mathrm{e}}/k_{\mathrm{B}}T^*_{\mathrm{e}}(t))^{3/2}\left(\frac{1}{\epsilon_\infty} - \frac{1}{\epsilon_0}\right)\exp\{z(t)/2\} \times \{[\nu_{\mathrm{LO}}(t) - (1 + \nu_{\mathrm{LO}}(t))\exp\{-z(t)\}]K_0(z(t)/2) - [\nu_{\mathrm{LO}}(t) + (1 + \nu_{\mathrm{LO}}(t))\exp\{-z(t)\}]K_1(z(t)/2)\}\mathbf{v}_{\mathrm{e}}(t), \tag{A.4}$$

where $z(t) \equiv \hbar\omega_{\mathrm{LO}}/k_{\mathrm{B}}T^*_{\mathrm{e}}(t)$, K_n are Bessel functions of the second kind, ϵ_0 and ϵ_∞ are the static and optic dielectric constants, and V is the volume of the system.

Finally, in equation (4), $J^{(2)}_{E_{\mathrm{LO}}}(t)$ is equal, but with a change of sign, to $J^{(2)}_{E_{\mathrm{e}}}(t)$, since it is the gain of energy of the LO phonons provided by the relaxing—through Fröhlich interaction—'hot' electrons.

References

[1] Pearson S J (ed) 1997 *GaN and Related Materials* (*Optoelectronic Properties of Semiconductors and Superlattices*) (New York: Gordon and Breach)
[2] Nakamura S and Fasol G 1997 *The Blue Laser Diode* (Berlin: Springer)
[3] Mohammad S N and Morkoç H 1996 *Prog. Quantum Electron.* **20** 361
[4] Akasaki I and Amano H 1997 *Japan. J. Appl. Phys.* **36** 5393

[5] Moore K and Trew R J 1997 *Mater. Res. Soc. Bull.* **22** 50
[6] Khan M A, Kuznia J N, Olson D T, Schaff W J, Burm J W and Shur M S 1994 *Appl. Phys. Lett.* **65** 1121
[7] Khan M A, Chen Q, Yang J W, Shur M S, Dermott B T and Higgins J A 1996 *IEEE Electron. Device Lett.* **17** 325
[8] Shur M S and Khan M A 1997 *Mater. Res. Bull.* **22** 44
[9] Chen Q, Yang J W, Gaska R, Khan M A, Shur M S, Sullivan G J, Sailor A L, Higgins J A, Ping A T and Adesida I 1998 *IEEE Electron. Device Lett.* **19** 44
[10] Shenai K, Scott R S and Baliga B J 1989 *IEEE Trans. Electron. Devices* **36** 1811
[11] Morkoç H, Cingolani R, Lambrecht W, Gil B, Jiang H-X, Lin J, Pavlidis D and Shenai K 1999 *MRS Internet J. Nitride Semicond. Res.* **4** U23–31
[12] Ferry D K 1974 *Phys. Rev.* **12** 2361
Littlejohn M A, Hauser J R and Glisson T H 1975 *J. Appl. Phys.* **26** 625
Kolník J, Oğuzman I H, Brennan K F, Wang R, Ruden P P and Wang Y 1995 *J. Appl. Phys.* **78** 1033
Shur M, Gelmont B and Khan M A 1996 *J. Electron. Mater.* **25** 777
O'Leary S K, Foutz B E, Shur M S, Bhapkar U V and Eastman L F 1998 *J. Appl. Phys.* **83** 826
Bellotti E, Doshi B K, Brennan K, Albrecht J D and Ruden P P 1999 *J. Appl. Phys.* **85** 916
[13] Ridley B K, Foutz B E and Eastman L F 2000 *Phys. Rev.* B **61** 16862
Orton J W and Foxon C T 1998 *Semicond. Sci. Technol.* **13** 310
Chin V W, Tansley T L and Osotchan T 1994 *J. Appl. Phys.* **75** 7365
Dhar S and Ghosh S 1999 *J. Appl. Phys.* **86** 2668
Look D C and Molnar R J 1997 *Appl. Phys. Lett.* **70** 3377
[14] Wraback M, Shen H, Carrano J C, Li T, Campbell J C, Schurman M J and Ferguson I T 2000 *Appl. Phys. Lett.* **76** 1155
Wraback M, Shen H, Carrano J C, Collins C J, Campbell J C, Dupuis R D, Schurman M J and Ferguson I T 2001 *Appl. Phys. Lett.* **79** 1303
Collazo R, Schlesser R, Roskowski A, Davis R F and Sitar Z 2000 *J. Appl. Phys.* **88** 5865
Collazo R, Schlesser R and Sitar Z 2002 *Appl. Phys. Lett.* **81** 5189
[15] Mansour N, Kim K W, Bannov N A and Littlejohn M A 1997 *Appl. Phys. Lett.* **81** 2901
[16] Foutz B E, Eastman L F, Bhapkar U V and Shur M S 1997 *Appl. Phys. Lett.* **70** 2849
[17] Caetano E W S, Costa Filho R N, Freire V N and Costa J A P 1999 *Solid State Commun.* **110** 469
[18] Foutz B E, O'Leary S K, Shur M S and Eastman L F 1999 *J. Appl. Phys.* **85** 7727
[19] Rodrigues C G, Freire V N, Vasconcellos A R and Luzzi R 2000 *Appl. Phys. Lett.* **76** 1893
[20] Luzzi R, Vasconcellos A R and Ramos J G 2002 *Predictive Statistical Mechanics: A Nonequilibrium Ensemble Formalism* (Dordrecht: Kluwer–Academic)
[21] Luzzi R, Vasconcellos A R and Ramos J G 2000 *Statistical Foundations of Irreversible Thermodynamics* (Stuttgart: Teubner–Bertelsmann Springer)
Luzzi R, Vasconcellos A R and Ramos J G 2001 *Riv. Nuovo Cim.* **24** 70
[22] Zwanzig R 1981 Where do we go from here? *Perspectives in Statistical Physics* ed H J Ravechè (Amsterdam: North-Holland)
[23] Rodrigues C G, Vasconcellos A R, Luzzi R and Freire V N 2005 *J. Appl. Phys.* **98** 043703
[24] Ramos J G, Luzzi R and Vasconcellos A R 1995 *Fortschr. Phys./Prog. Phys.* **43** 265
Bomfim C, Ramos J G, Vasconcellos A R and Luzzi R 2007 as yet unpublished
[25] Grad H 1958 Principles of the kinetic theory of gases *in Handbuch der Physik XII* ed S Flügge (Berlin: Springer)
[26] Starikov E, Shiktorov P, Gruinskis V, Varani L, Vaissière J C, Palermo C and Reggiani L 2005 *J. Appl. Phys.* **98** 083701
[27] Collazo R, Schlesser R, Roskowski A, Davis R F and Sitar Z 2000 *J. Appl. Phys.* **88** 5865
[28] Casas-Vasquez J and Jou D 2003 *Rep. Prog. Phys.* **66** 1937
[29] Rodrigues C G, Vasconcellos A R and Luzzi R 2000 *Transp. Theory Stat. Phys.* **29** 733
Rodrigues C G, Vasconcellos A R, Luzzi R and Freire V N 2005 *J. Appl. Phys.* **98** 043702
[30] Lauck L, Vasconcellos A R and Luzzi R 1990 *Physica* A **168** 789
[31] Algarte A C, Vasconcellos A R and Luzzi R 1992 *Phys. Status Solidi* b **173** 487
[32] Madureira J R, Vasconcellos A R, Algarte A C and Luzzi R 1998 *Phys. Rev.* E **57** 3637